

Water stress induced breakdown of carbon-water relations: indicators from diurnal FLUXNET patterns

Jacob A. Nelson, Nuno Carvalhais, Mirco Migliavacca, Markus Reichstein, Martin Jung

Abstract

Understanding of terrestrial carbon and water cycles is currently hampered by an uncertainty in how to capture the large variety of plant responses to drought. In FLUXNET, the global network of CO₂ and H₂O flux observations, many sites do not uniformly report the ancillary variables needed to study drought response physiology. To this end, we outline two data-driven indicators based on diurnal energy, water, and carbon flux patterns derived directly from the eddy covariance data and based on theorized physiological responses to hydraulic and non-stomatal limitations. Hydraulic limitations (i.e. intra-plant limitations to water movement) are proxied using the relative diurnal centroid (C_{ET}^*), which measures the degree to which the flux of evapotranspiration (ET) is shifted toward the morning. Non-stomatal limitations (e.g. inhibitions of biochemical reactions, RuBisCO activity, and/or mesophyll conductance) are characterized by the Diurnal Water:Carbon Index (DWCI), which measures the degree of coupling between ET and gross primary productivity (GPP) within each day. As a proof of concept we show the response of the metrics at 6 European sites during the 2003 heatwave event, showing varied response of morning shifts and decoupling. Globally, we found indications of hydraulic limitations in the form of significantly high frequencies of morning shifted days in dry/Mediterranean climates and savanna/evergreen plant functional types (PFT), whereas high frequencies of decoupling were dominated by dry climates and grassland/savanna PFTs indicating a prevalence of non-stomatal limitations in these ecosystems. Overall, both the diurnal centroid and DWCI were associated with high net radiation and low latent energy typical of drought. Using three water use efficiency (WUE) models, we found the mean differences between expected and observed WUE to be -0.09 to 0.44 umol/mmol and -0.29 to -0.40 umol/mmol for decoupled and morning shifted days respectively compared to mean differences -1.41 to -1.42 umol/mmol in dry conditions, suggesting that morning shifts/hydraulic responses are associated with an increase in WUE whereas decoupling/non-stomatal limitations are not.

Introduction

Processes such as photosynthesis and transpiration are so intimately linked that knowledge and assumptions about one process are needed to accurately understand the other. Unfortunately, the relationship between carbon and water cycles

27 is not fully understood [47], passing the biases and uncertainties caused by an incomplete carbon:water framework back
28 onto flux estimates specifically and global water and carbon cycle interactions and dynamics in general [18, 46, 15]. One
29 source of uncertainty that is increasingly being identified is the diverse responses of plants to water limitation [55, 9,
30 44], which hampers the understanding and predictability of water and carbon cycles during drought. Here we outline
31 potential causes of uncertainty in carbon:water dynamics in an effort to outline data-derived inductors based on current
32 theory.

33 Classically, vegetation water and carbon fluxes are linked by stomates, where an open stomate allows CO₂ to enter the leaf
34 and, consequentially, water is lost. Most theoretical frameworks make some form of assumption that carbon assimilation
35 (A) and water losses (T) are both contingent primarily on leaf stomatal conductance (g_s). This assumed relationship
36 allows us to pass between the realms of carbon and water, based on the assumption that at any given time both A and T
37 are proportional to the stomatal conductance multiplied by the difference in internal and external CO₂ and water vapor
38 concentrations. More specifically,

$$A = g_s \cdot \Delta c \quad \text{and} \quad T = 1.6 \cdot g_s \cdot \Delta v \quad (1)$$

39 where Δc and Δv are the differences in inner and outer stomatal cavity concentrations of CO₂ and water vapor, respec-
40 tively. These diffusion equations lead to the relatively consistent carbon:water ratio, generally expressed as a water use
41 efficiency ($WUE = A/T$). At the ecosystem level where direct measurements of A and T are not available, WUE is sim-
42 ply calculated as the ratio of gross primary productivity (GPP) to total evapotranspiration (ET) [22]. These carbon:water
43 links are fundamental to understanding how stomata are regulated and underly key functioning in mechanistic plant and
44 ecosystem models. One such set of models are those based on optimality theory which posit that plants tend to optimize
45 carbon gains to water losses, such as those described by Katul et al. [17] and Katul, Palmroth, and Oren [16]. These
46 concepts from Katul, which carry the assumptions of RuBisCO (light) limitation, were built upon by Zhou et al. [54] and
47 Zhou et al. [52] to give the equation,

$$uWUE = \frac{GPP \cdot \sqrt{VPD}}{ET} \quad (2)$$

48 where the \sqrt{VPD} accounts for the stomatal response to vapor pressure deficit (VPD) assuming stomatal response op-
49 timizes carbon gain to water losses. Accounting for the VPD response allows for a more stable metric of WUE that is
50 temporally more stable and physiologically more meaningful, such as when comparing the diurnal cycles of carbon and
51 water. As ET is the sum of both T and non-biological evaporation (e.g. soil and intercepted evaporation), often periods
52 during and shortly after rain events are excluded from WUE estimates to minimize the influence of non-plant evapora-

53 tion. Ultimately, calculations of WUE provide a simple summary of the cost in water per carbon gain and becomes an
54 indicator for how plants have and will adapt to the physical limitations of their changing environments [18, 47].

55 Though assuming a rigid carbon:water relationship works well in conditions when ecosystems are moderately wet, con-
56 ditions associated with the majority of carbon and water fluxes, an inflexible carbon:water assumption is unsatisfactory
57 in that these assumptions may breakdown as plants shift from light to water limitations. Indeed, in a review of leaf level
58 stomatal conductance models, Damour et al. [7] concluded that the majority of stomatal models fail to adequately capture
59 the effects of drought. This failure to capture the effects of drought is not only disconcerting as water limited conditions
60 are when ecosystems are most at risk, but an incomplete framework tends to propagates errors and uncertainties from
61 models into estimates of the water and carbon cycles. For instance, in outlining a road map for improved modeling of
62 photosynthesis, Rogers et al. [44] noted as key recommendations both improving information about water:carbon re-
63 lations (in the form of the stomatal slope parameter g_1) as well as improving understanding of the response of carbon
64 assimilation to drought. Similarly, in an analysis of parameter uncertainties for a terrestrial biosphere model, Dietze
65 et al. [9] found that two of the top five parameters contributing to the predictive uncertainty of net primary productivity
66 were associated with plant water regulation. This uncertainty is reflected in the stomatal conductance parameterization
67 exercise from Knauer, Werner, and Zaehle [19], where the authors were able to improve model performance in predicting
68 EC measured GPP and ET by including atmospheric effects (in the form of VPD) on stomatal conductance, but concluded
69 that further improvement required global understanding of water limitation response variation across plant functional
70 traits and growing conditions, which is currently unavailable.

71 Two ideas to account for the errors in carbon:water assumptions under dry conditions have begun to emerge: that hy-
72 draulic limitations in transporting water from root to leaf change stomatal responses and thus limit transpiration under
73 high demand, or that changes in the intra-leaf processes of carbon transport and fixation under drought conditions result
74 in non-stomatal limitations that impact carbon assimilation independently of water fluxes [34].

75 As soil water potentials in the root zone become increasingly negative, the long-term plant strategy may turn from op-
76 timizing carbon fixation to preventing damage to hydraulic architecture [48]. As such, stomata and transpiration are
77 likely to increasingly respond not just to atmospheric conditions, but also soil moisture. Under this hydraulic limitation
78 framework, a plant will be reacting to the inability to transport water, even though the key control mechanism for a plant
79 is via the stomata, possibly expressed as an increase in sensitivity. Such assumptions are consistent with the mechanisms
80 encoded in some land surface and ecosystem models, which account for water limitations by scaling the water to carbon
81 ratio in relation to available soil moisture. Though this method should link the leaf physiology to the soil and thus cap-
82 ture some hydraulic limitation, it has been criticized for not capturing the variety of drought responses found in different
83 plant species and ecosystems [8]. This diversity in plant responses has been pointed to as a key point of uncertainty in
84 earth system models [9].

85 Though ecosystem water and carbon fluxes are predominantly controlled by stomates, non-stomatal or bio/photo-
86 chemical inhibitions to carbon assimilation are worth considering as they have the capacity to decouple the water-carbon
87 exchange. This decoupling could include conditions where the stomates are transpiring water but intra-leaf factors are
88 slowing carbon fixation, changing the intrinsic water use efficiency directly. Intra-leaf factors could include effects such
89 as production of reactive oxygen species [23]; environmental limitations to the photosynthetic pathways, such as leaf
90 temperature [31]; or declines in mesophyll conductance [11]. Non-stomatal limitations have been observed at ecosystem
91 scale [42, 32], though the exact mechanism is difficult to elucidate [40]. These effects likely vary between species, as
92 well as with the rate of onset of drought, access to water, and other environmental conditions.

93 **Objectives**

94 There seems to be a collective conclusion that the breakdown of carbon:water assumptions needs to be better character-
95 ized in general, and specifically for implementation in modeling frameworks [De Kauwe et al. [8]; Manzoni [25]; Zhou
96 et al. [55]; Flexas et al. [11]; Egea, Verhoef, and Vidale [10];]. Though the problem is becoming clear, the way forward
97 is hampered by an uncertainty in how to capture the large variety in the response to drought across climates, strate-
98 gies, and species. In this sense, the use of EC measured diurnal patterns of carbon, water, and energy fluxes to derive
99 clues on ecosystem drought responses at a daily resolution could prove valuable both as a means to identify potential
100 periods of ecosystem stress, inform machine learning algorithms on ecophysiological conditions not found in environ-
101 mental variables, as well as benchmarking a models ability to capture sub-daily dynamics. To this end, we propose two
102 data-driven indicators of water stress, the diurnal water:carbon index (DWCI) and the relative diurnal centroid in LE
103 (C_{ET}^*). Both metrics are derived directly from the EC data and based on expected physiological responses to hydraulic
104 and non-stomatal limitations. Using these data-driven indicators we then characterize the distribution of these limita-
105 tions across a global spread of climate and vegetation types. Finally, we explore the ability of these indicators to detect
106 the disagreements between modeled and observed water use efficiency, and explore how these biases may be attributed
107 to hydraulic and non-stomatal limitations.

108 **Methods and Materials**

109 **Data**

110 Carbon, water, and every fluxes measured with EC, as well as meteorological data, were obtained from the 2007
111 FLUXNET La Thuile Synthesis Dataset [12]. Half-hourly latent heat and net ecosystem exchange (NEE) fluxes were
112 collected and processed using standard QA/QC procedures [36], gap-filling and partitioning algorithms [41]. From the

113 database, half-hourly gross primary productivity (GPP) and ET data (derived from latent heat flux measurements) were
114 downloaded and used for the following analysis. An interactive map of sites used can be found in File S1.

115 In order to provide a consistent measure of ecosystem dryness that can be utilized across sites, the ratio of water evapo-
116 rated to potential water evaporated was calculated as evaporative fraction (EF), or the fraction of actual ET to Potential
117 ET (PET). PET was calculated as the daily fraction between the measured ET and estimated ET via a Priestly-Taylor
118 model [38] using site measured net radiation (Rn) and air temperature (T_{air}). The slope (alpha parameter) was fit for
119 each site-year using 95th quantile regression [20] instead of using the original 1.26 value derived for a “well watered
120 crop” [38].

121 In order to get high quality data and minimize the influence of abiotic evaporation (hereafter just evaporation), all data
122 was filtered with the aim to include only non-gap filled data in the growing season with dry surface conditions. Growing
123 season was defined as all days where $GPP > 1 \text{ gC} \cdot \text{m}^{-2} \cdot \text{d}^{-1}$ and daily mean air temperature $> 5 \text{ }^\circ\text{C}$. These threshold were
124 shown to give good response in the proposed metrics while minimizing variability due to low diurnal signals, a sensitivity
125 analysis of which can be found in supplementary Figure S2. In an effort to minimize contributions of evaporation, the
126 conservative soil wetness index (CSWI) was employed which was designed to estimate whether the ecosystem is likely to
127 have “dry” surfaces and therefore ET is likely to be dominated by transpiration. This approach requires a certain amount
128 of evaporation to occur after a rain event before the surface is considered to be “dry” and can be contrasted to the method
129 of removing a set time period after rain employed in previous studies [30, 2, 18]. CSWI is calculating by first quantifying
130 the storage at time t (S_t) as,

$$S_t = \min(S_{t-1} + P_t - ET_t, S_o) \quad (3)$$

131 where ET_t and P_t are the ET and precipitation at time-step t respectively, S_t is effectively capped at a maximum storage
132 value of S_o , which was set to 5 mm. Furthermore, to make the metric conservative in regards to assumed water inputs,
133 any precipitation event will refill the storage from 0 mm,

$$CSWI = \max(S_t, \min(P_t, S_o)) \quad (4)$$

134 which has the effect of requiring all precipitation up to 5 mm to be evaporated from the system before negative storage
135 can occur. Any gaps in the precipitation data were assumed to be a precipitation event of 5 mm in order to prevent
136 any unmeasured precipitation from biasing the results by inadvertently including rainy days. Code and further outline
137 of the algorithm can be found in File S3 as well as at Nelson [33]. Evaporation was assumed to be negligible when
138 $CSWI < 0$. This method was used over the more standard method of removing 1-5 days after a rain event, as it does not

139 make the assumption that the surface will dry in a fixed amount of time, instead relying on a minimum amount of ET.
 140 As a comparison, the median time period for the CSWI to go from fully wet (CSWI=5) to “dry” (CSWI<=0) was 3.5 days
 141 across all sites in summer, where summer was defined as the period when daily potential radiation above median daily
 142 potential radiation for each site.

143 The data filtering as outlined in this section was designed to isolate periods firmly in the growing season when plants are
 144 active and the signal of ET is most likely to be dominated by plant controls.

145 **Relative diurnal centroid (C_{ET}^*)**

146 As soils dry, it becomes more difficult to transport stem and root zone moisture to the leaf, potentially causing hydraulic
 147 limitations for the plant to transport water. This shift was seen in eddy covariance data in a study by Wilson et al. [50],
 148 who examined the shift of latent compared to sensible heat, which suggested that a shift in water fluxes towards dawn
 149 can be indicative of afternoon stomatal closure. Shifts were further explored in a modeling study by Matheny et al. [29]
 150 which found that the morning shift was not well captured by models and attributed the errors to inadequate hydraulic
 151 limitations in the models. The daily cycle of wetting and drying acts as a capacitor in the hydraulic circuit, allowing water
 152 stores to be more easily transported in the morning and depleting in the afternoon. As bulk soil moisture declines, this
 153 effect may be strong enough to shift the diurnal cycle of ET significantly toward the morning. Quantifying diurnal shifts
 154 in EC data using the diurnal centroid was first explored by Wilson et al. [50]: defined as the flux weighted mean hour, or

$$C_{flux} = \frac{\sum flux_t \cdot t}{\sum flux_t} \quad (5)$$

155 where t is a regular, sub-daily time interval (here t measures as decimal hour at half-hourly time-step). The resulting
 156 C_{flux} is the weighted mean hour of the diurnal cycle of that particular flux for that particular day. For example, if a
 157 calculated C_{ET} for a given day (using measurements of decimal hour) equals 12.25, this would entail that the weighted
 158 mean for that day is 15 minutes past noon. Figure 1 shows an example of the shifts in the monthly average cycle from
 159 a wet month to a dry month. In order to isolate a shift, we then had to control for variations in global radiation (R_g),
 160 both fluctuations due to clouds and differences in the timing of solar noon. Therefore, the difference between the diurnal
 161 centroids of ET (C_{ET}) and R_g (C_{R_g}) was calculated as

$$C_{ET}^* = C_{R_g} - C_{ET} \quad (6)$$

162 giving C_{ET}^* as the diurnal centroid of ET relative to R_g . The resulting values of C_{ET}^* are not tied to the carbon cycle, which

163 can be affected by non-stomatal limitations and generally shows a more prominent midday depression. Annotated code
 164 for the CSWI calculation can be found in File S4 as well as at Nelson [33]. Though a diurnal centroid can be calculated
 165 for any diurnal cycle, basing a metric on the morning shift of ET relative to Rg has the advantage of targeting the non-
 166 atmospheric drivers of the water flux, of which there are few ancillary variables.

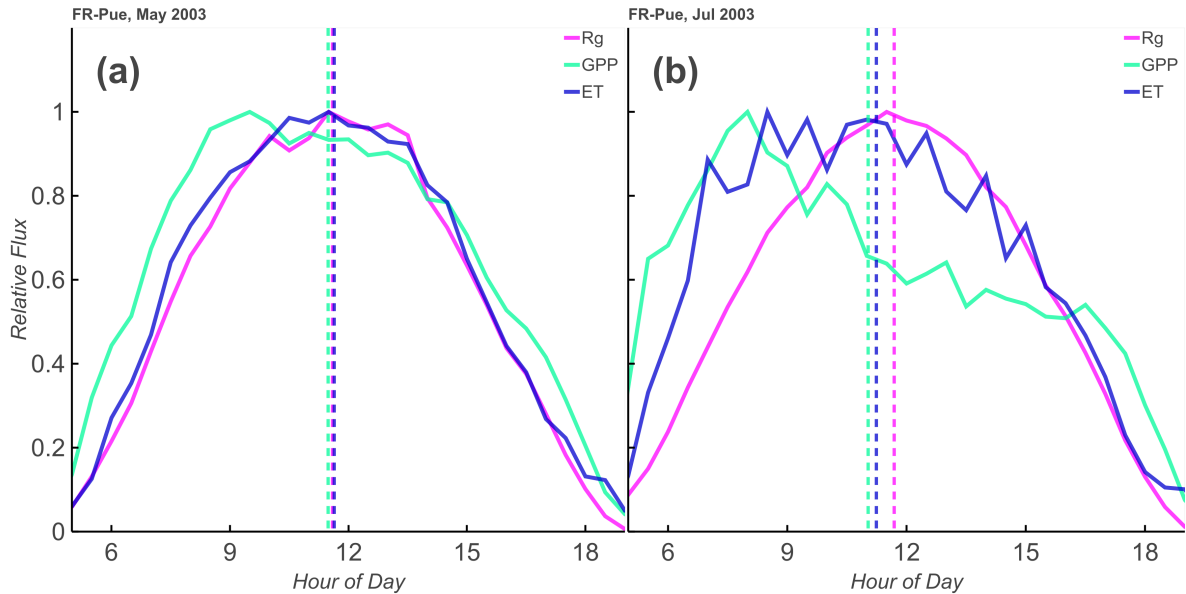


Figure 1: One month average cycle (solid lines) and accompanying diurnal centroid (vertical dashed lines) of incoming shortwave radiation (Rg), evapotranspiration (ET), and gross primary productivity (GPP) at the Peuchabon, France ('FR-Pue') site during 2003. May is relatively wet (32 mm rainfall, left) and July is relatively dry (0 mm rainfall, right). While ET and Rg correspond well in the wet month, the dry month shows a distinct phase shift in both GPP and ET fluxes towards the morning, as well as a midday depression in GPP.

167 Diurnal water carbon index (DWCI)

168 If transpiration and carbon assimilation are predominantly controlled by stomatal conductance, it follows that their
 169 diurnal cycles should be largely in sync. In other words, regardless of a plants maximum T or A, if the stomates start to
 170 close, both rates should be decrease by a similar percentage. On the other hand, non-stomatal limitations that inhibit
 171 carbon assimilation independent of water have the capability to alter the diurnal cycle on just one flux, causing them to
 172 decouple. In an effort to quantify the degree of carbon:water coupling for an individual day, we examined the relationship
 173 of GPP and ET, where,

$$ET \propto GPP \cdot \sqrt{VPD} \quad (7)$$

174 or,

$$ET = i \cdot GPP \cdot \sqrt{VPD} \quad (8)$$

175 This relationship incorporates the assumption that, at least over short time scales, the amount of carbon that enters
 176 the leaf is proportional to the amount of water that leaves, and also incorporates the non-linear response of stomates
 177 to VPD [17, 16, 54]. This model, though simple, has been shown to work well across a variety of EC sites [52]. Figure 2
 178 (upper panels a,b) shows a comparison between the daily cycles in a wet and dry month. By calculating a daily correlation
 179 between the normalized daily cycles of ET and $GPP \cdot \sqrt{VPD}$, we come to a correlation coefficient for each day (see
 180 Figure 2, lower panels c,d). For well watered days in the growing season the two signals tend to be well correlated ($\rho > 0.9$),
 181 but tends to be less correlated in periods of stress, a comparison of which can be seen in Figure 2 (lower).

182 As it is, this daily correlation coefficient is dependent on the signal strength, or magnitude, of the flux. Low correlation
 183 values could just as easily be from carbon:water decoupling as to a low signal to noise ratio. Therefore, to produce a more
 184 robust metric and account for these statistical decreases in correlation, we turned the daily correlation coefficient into
 185 an index based on its rank in a distribution of correlation coefficients from artificial datasets. These artificial datasets
 186 are constructed using the diurnal signal from potential radiation, with Gaussian noise ($\mathcal{N}(0, \sigma)$) added according to the
 187 standard deviation random uncertainty of the ET and NEE fluxes, or

$$LE_{artificial} = \frac{Rg_{pot}}{Rg_{pot}} \cdot \overline{LE} + \mathcal{N}(0, \sigma_{LE|NEE}^2) \quad (9)$$

188 and

$$NEE_{artificial} = \frac{Rg_{pot}}{Rg_{pot}} \cdot \overline{NEE} + \mathcal{N}(0, \sigma_{NEE|LE}^2) \quad (10)$$

189 Uncertainties of the NEE and ET fluxes were estimated from the gap filling procedure of Reichstein et al. [41], with
 190 the uncertainty equal to the standard deviation of flux measurements within a time window and similar meteorological
 191 conditions. As GPP is calculated from gap-filled values of NEE, the uncertainty from NEE was used for GPP. Furthermore,
 192 the correlation structure between the noises in LE and and NEE was preserved in the artificial dataset.

193 In essence, by using the underlying signal from potential radiation, both the artificial ET and $GPP \cdot \sqrt{VPD}$ are perfectly
 194 correlated when no noise is added. Adding noise then isolates the decoupling effect of signal to noise ratio. An artificial
 195 correlation coefficient can then be calculated from the two artificial datasets in the same manner as from the real dataset,
 196 and this experiment is repeated 100 times for each day, giving a daily distribution of artificial correlation coefficients. The
 197 rank of the real correlation coefficient in the distribution from the artificial set gives a probability that the carbon and

198 water signals are actually coupled. The resulting index has a range of 0-100, with 100 indicating that the real correlation
 199 coefficient was greater than the entire artificial set, and therefore it is very likely that carbon and water are coupled. From
 200 this index we can now quantify if the water and carbon signals are coupled for any given day, and therefore shed light onto
 201 whether the two fluxes are only controlled by the opening and closing of stomates. Annotated code for this calculation
 202 can be found in File S5 as well as at Nelson [33].

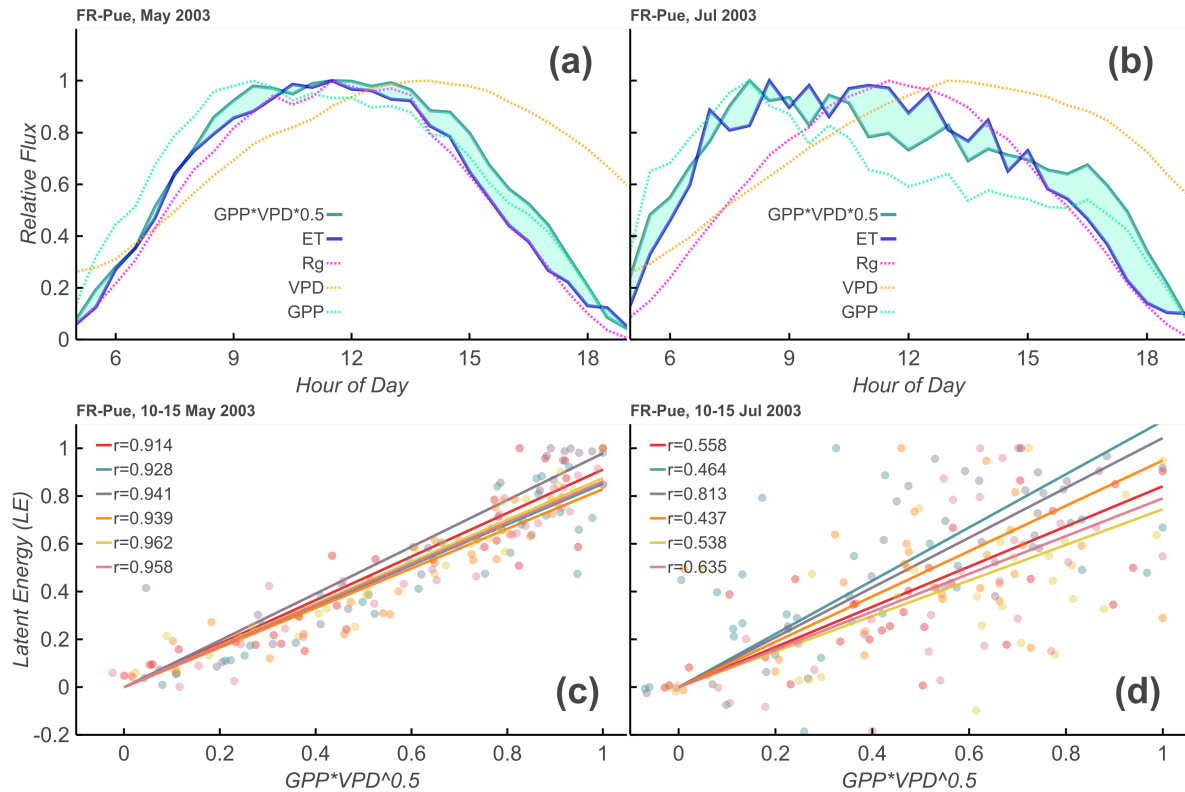


Figure 2: Theoretical overview of diurnal water carbon index upper panels: One month average diurnal cycle of incoming shortwave radiation (R_g), evapotranspiration (ET), vapor pressure deficit (VPD), gross primary productivity (GPP), and $GPP*VPD^{-0.5}$ at the Peuchabon Forest, France (‘FR-Pue’) site during 2003. Discrepancies between $GPP*VPD^{-0.5}$ and ET increase from the relatively wet May (32 mm rainfall, left) to the relatively dry July (0 mm rainfall, right). lower panels: These discrepancies are reflected in the daily correlation values between $GPP * VPD^{-0.5}$ and ET, giving an indication of the appropriateness of the uWUE model for each day, as well as the degree of coupling between water and carbon signals.

203 Models and parameter estimation

204 In order to benchmark whether these metrics are capturing information that is possibly not being captured in modern
 205 model frameworks, three simple models were used to estimate WUE (GPP/ET) for each day at each site and compared
 206 to actual flux data. The purpose of the exercise was to evaluate if bias in the model predictions were associated with
 207 decoupled or morning shifted days, thus indicating that the metrics are corresponding to information that the models
 208 are unable to capture. Here we utilize three models to provide a spectrum of theoretical to empirical basis. The ‘Katul-

209 Zhou” model, as defined and used in calculation of the DWCI, is based in stomatal optimization theory [17, 16, 52], which
 210 makes the assumption that the WUE is constant if corrected by the effect of VPD, using an inverse square root as the
 211 assumed relationship. Though the constant nature of uWUE may not be correct, with the optimal carbon cost of water
 212 changing over day or weeks [26, 35], a yearly parameter of uWUE was estimated which is consistent with other modeling
 213 exercises [53]. One step away from a theoretical basis is a revision of this model by Boese et al. [3], the “Boese” model,
 214 where an additional radiation term was added such that,

$$ET = i \cdot GPP \cdot \sqrt{VPD} + r \cdot Rg \quad (11)$$

215 where i and r are parameters fit to each site-year. This relationship with Rg was shown to have a better predictive per-
 216 formance for EC data from 115 sites [3]. The interpretation of this extra radiation term is not clear and is difficult to
 217 reconcile with the current understanding of physiology. It is possible the term could be related to biophysical effects,
 218 e.g. VPD at leaf surface vs the measured ambient VPD. Nevertheless, the Boese model is an empirical and ecosystem
 219 scale model that complements the theoretical and originally leaf-level model from Katul-Zhou.

220 Parameters of these models were estimated for each site-year. The Boese model parameters were fit using trimmed least
 221 squares regression (TLS) which minimizes the 90th percentile of SSE to prevent influence of large outliers [45, 43]. As the
 222 error in both ET and GPP are assumed to be of similar magnitude, the i parameter in the Katul-Zhou model was calculated
 223 using geometric mean regression, where the final slope was calculated as the geometric mean of the parameters from

$$ET = i_{GPP} \cdot GPP \cdot \sqrt{VPD} \text{ and } GPP \cdot \sqrt{VPD} = \frac{ET}{i_{ET}} \quad (12)$$

224 Both the Katul-Zhou and Boese models are theoretically based and here implemented have the underlying assumptions
 225 of RuBisCO-limited conditions and constant carbon cost of water throughout the season which may not reflect reality.
 226 Therefore a fully empirical and highly non-linear model can give insight into how much information is actually stored
 227 in the data while minimizing any assumptions. As a fully empirical model, a random forest regression (RandomFore-
 228 stRegressor from Pedregosa et al. [37] based on Breiman [4]) was fit to half-hourly ET data for each site using Rg , VPD,
 229 T_{air} , GPP and year as input parameters. Values were estimated using 50 trees with predictions made using out-of-bag
 230 estimates to prevent over-fitted model predictions.

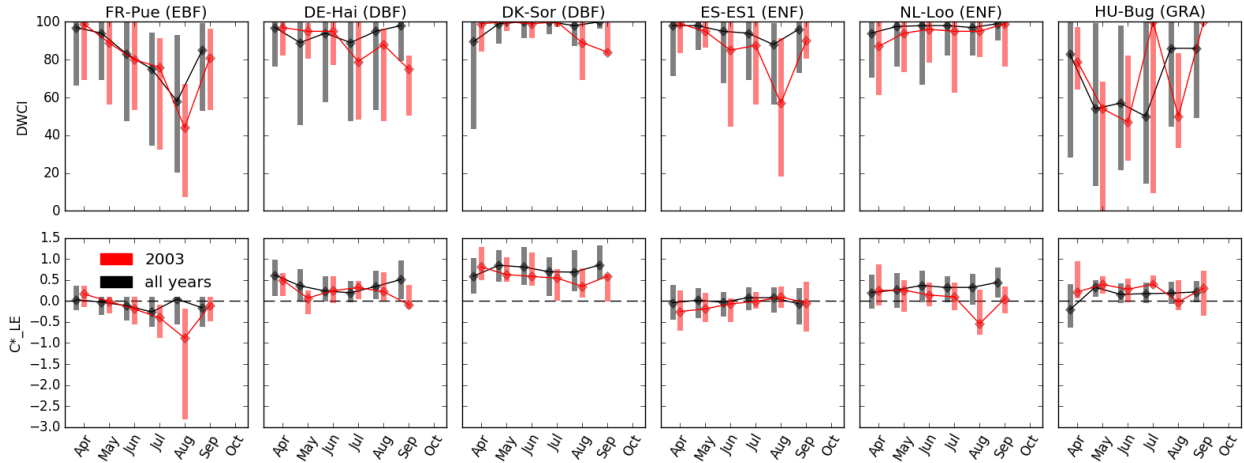


Figure 3: Monthly median diurnal water carbon index (DWCI, lower panels) and diurnal centroids (C_{ET}^* , upper panels) for 6 sites in Europe. Data from all years available (black) is compared to 2003 (red) during which a drought event resulted in high temperatures and low precipitation throughout the summer. Note DWCI of 0-100 indicate lowest-highest probability of diurnal carbon:water coupling and C_{ET}^* of -1 to 1 indicate one hour morning shifted to one hour afternoon shifted ET. Vertical bars represent interquartile range. Sites from 4 plant functional types: evergreen broadleaf (EBF), deciduous broadleaf (DBF) and evergreen needleleaf (ENF) forests, as well as grasslands (GRA). Ecosystems show tendencies of morning shifts (e.g. DK-Sor and NL-Loo) and carbon:water decoupling (e.g. ES-ES1 and HU-Bug) during the drought year.

231 Results

232 As a case study, C_{ET}^* and DWCI time-courses for six sites from Europe are shown in Figure 3, with an emphasis on
 233 2003 when the continent was struck by a heatwave that was shown to effect both the carbon and water cycles [6, 39,
 234 13]. For DWCI, forest sites showed high water:carbon coupling throughout the growing season, with the exception of
 235 Peuchebon (FR-Pue) which showed a regular seasonal cycle of decoupling. The grassland site (HU-Bg) showed a higher
 236 variability in DWCI compared to the forest sites (all others). All sites showed either a decrease in median DWCI or an
 237 increase in variability during 2003, generally in July or August, particularly at Hainich (DE-Hai), Bugacpuszta (HU-
 238 Bug), and El Saler (ES-ES1). This increase in decoupling during 2003 is consistent with the hypothesis of non-stomatal
 239 limitations being expressed in hot, dry conditions which can affect carbon fixing mechanisms. Median diurnal centroid
 240 values across all years varied in absolute magnitude, but were generally near or above zero, i.e. the water cycle showed
 241 no shift or an afternoon shift. One exception would be the Mediterranean oak forest of Peuchabon, which shows a slight
 242 seasonal cycle of morning shifts going from a slight afternoon shift to a slight morning shift during June, July, and
 243 August. During drought years, sites that showed distinctive morning shifts were Peuchabon (FR-Pue), Soroe (DK-Sor),
 244 and Loobos (NL-Loo). The framework that morning shifts are associated with water stress from soil moisture depletion
 245 would be supported by the increase in morning shifts during 2003, though factors such as species composition and access
 246 to soil water would play a significant role and could account for the differences among sites. All sites had significantly
 247 different ($p < 0.05$, Wilcoxon rank-sum test) DWCI values between 2003 and all other years except Peuchabon, whereas

248 with C_{ET}^* only Puechabon, Soroe, and Loobos showed significant differences.

249 **Distribution of data driven indicators by vegetation type and climate**

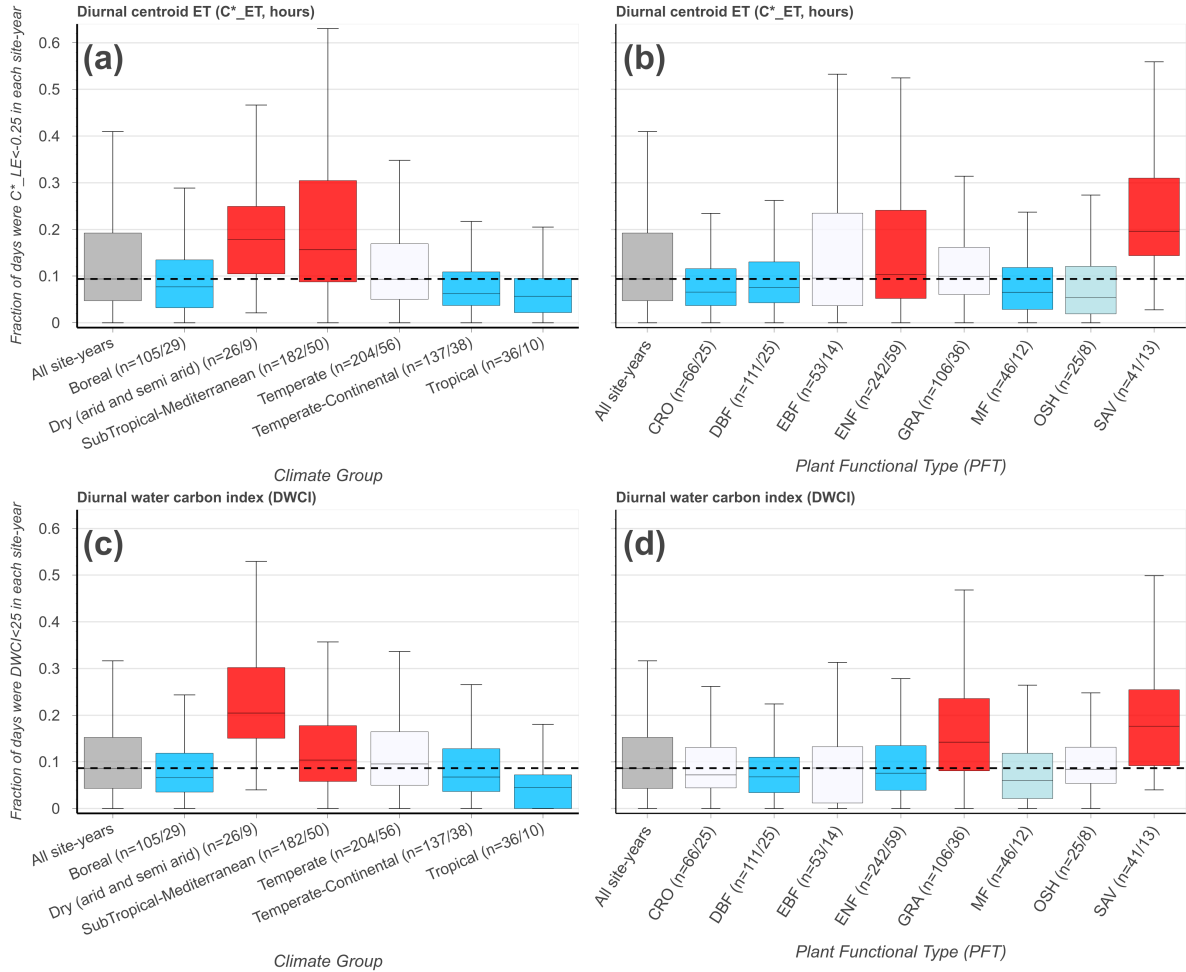


Figure 4: The frequency of morning-shifted Diurnal Centroids ($C_{ET}^* < -0.25$ hours, upper panels a,b) and low diurnal water carbon index (DWCI < 25, lower panels c,d) for 690 fluxnet site-years/192 sites, grouped by climate group (left panels a,c) and plant functional type (right panels b,d). Group labels on x-axis indicate the number of site-years/sites (n =site-years/sites) for each category. Dashed line is the median for all site-years. Color shade indicates level of significance, with light colors and dark colors having p-values < 0.10 and < 0.05 respectively (Wilcoxon–Mann–Whitney two-sample rank-sum test), red and blue colors indicate distributions higher and lower respectively compared to data from all sites excluding the group. Only sites-years with at least 20 data points and groups with more than 5 site-years were included.

250 The frequency of low values of diurnal centroid and DWCI across climate groups and plant functional types is shown
 251 in Figure 4. The thresholds designating decoupling and morning shifts were 25 and -0.25 for DWCI and C_{ET}^* respec-
 252 tively. These thresholds were chosen to highlight frequency differences between sites and were shown to have large
 253 metric responses under dry conditions while having low frequencies under wetter conditions (see sensitivity analysis in
 254 supplementary Figure S2). Furthermore, these thresholds results in a similar median frequency of uncoupled and morn-

255 ing shifted days between all site-years being 8.7% and 9.4% of days respectively. The similarity in median frequencies
256 across site-years allowed for easier inter-comparison between the two metrics. The frequency of decoupling and morn-
257 ing shifts using these thresholds for each site can be found in the map found in File S1. Though there is a fairly large
258 variance across climate groups and plant functional types, low values of both DWCI and C_{ET}^* occur at higher frequen-
259 cies in savanna ecosystems and dry or Mediterranean climates. Conversely, lower frequencies of both metrics are seen
260 in tropical, boreal, and temperate-continental climates. Strikingly, the arid and semi-arid climate group seems to be
261 associated with the majority of low DWCI occurrences, with a median frequency of about 20% of days being uncoupled
262 between site-years. Overall, frequencies were highly variable within plant functional types. Interestingly, C_{ET}^* seems
263 to be more variable in moderately dry ecosystems with potentially deep roots, favoring woodier savannas and evergreen
264 needle-leaf forests over grasslands and open shrub lands. In contrast, DWCI shows similarly high frequencies from sa-
265 vannas and grasslands. The differing responses between tree and grass dominated ecosystems can be further seen in
266 Figure 5, where savanna and grassland ecosystems show a distinct decrease in DWCI under conditions of low EF, in con-
267 trast to the forested sites which show a higher degree of carbon:water coupling, though still a slight decrease. Forested
268 ecosystems show a higher degree of morning shift under low EF conditions when compared to grasslands, with savannas
269 being somewhere between the two.

270 The response of both variables to drought stress is further observed in Figure 6, where low mean values of both DWCI
271 and C_{ET}^* are associated with conditions of high net radiation and low latent energy, indicative of drought. As this figure
272 includes all days from all sites which meet the filtering outlined in the Data subsection of the Methods, i.e. dry periods
273 in the growing season, these figures exhibit the universality of the metrics across climates, ecosystems, and time periods.
274 This pattern is much cleaner with the diurnal centroid than with DWCI, though mean values are generally above 50 for
275 most bins, indicating that most days are well coupled. Low values of both indicators are also seen under conditions
276 with low Rn and high latent energy (as seen by the dark streak at the top edged in Figures 6c,e), which is generally not
277 associated with drought stress. Further analysis showed that these points are also associated with energy balance over
278 closure, where the sum of latent and sensible heat is greater than net radiation ($ET+H>Rn$, see Figure S2) and therefore
279 likely represent a data problem rather than a physiological response. Removing all days where the energy balance is
280 over closed did not alter the patterns associated with drought. Apart from the response to periods of high LE and low
281 Rn, the metrics showed diverging response when looking at EF (ET/PET which is similar to LE/Rn) and VPD, with
282 DWCI showing a much stronger response to VPD and C_{ET}^* showing a much stronger response to EF (Figure 6a,d). This
283 difference in response would indicate that DWCI is more responsive to atmospheric demand (estimated via VPD) and
284 C_{ET}^* is more responsive to water limitations. Both DWCI and C_{ET}^* also show a trend with low GPP, although in the case
285 of the diurnal centroid the effect is limited to both low GPP and ET (Figure 6c,g).

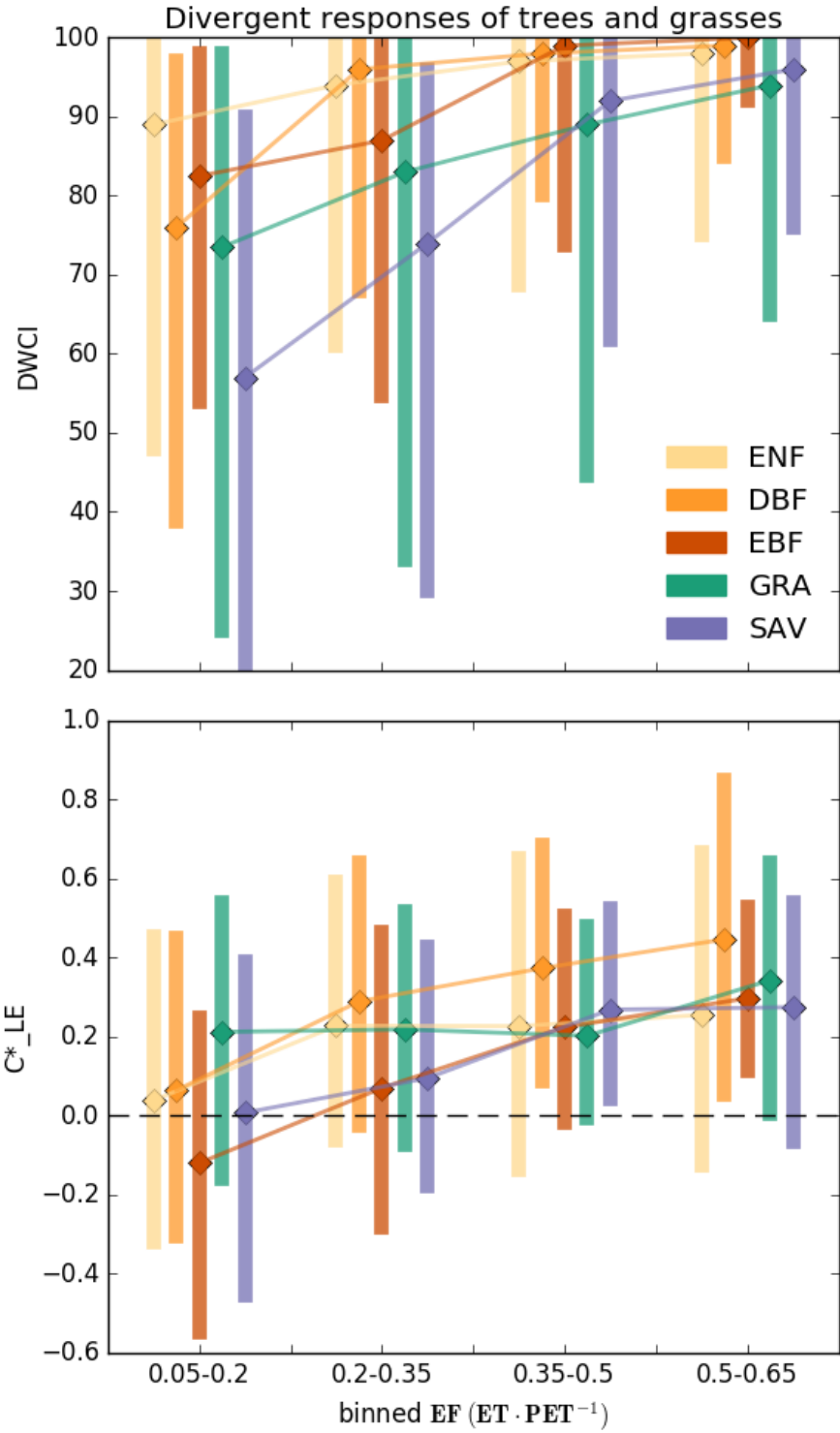


Figure 5: Median diurnal water carbon index (DWCI, upper panel) and diurnal centroid (C_{ET}^* , lower panel) of plant functional types binned by evaporative Fraction (EF, low values indicate dry conditions). Note DWCI of 0-100 indicate lowest-highest probability of diurnal carbon:water coupling and C_{ET}^* of -1 to 1 indicate one hour morning shifted to one hour afternoon shifted ET. Evergreen needleleaf (ENF), deciduous broadleaf (DBF), and evergreen broadleaf (EBF) forests show increased morning shifts (low C_{ET}^*) with decreasing EF when compared to grassland (GRA) sites which tended to have decreased carbon:water decoupling (low DWCI) with decreasing EF. Savanna ecosystems (SAV) show a high degree of decoupling and intermediate levels of morning shifts. Vertical bars represent interquartile range.

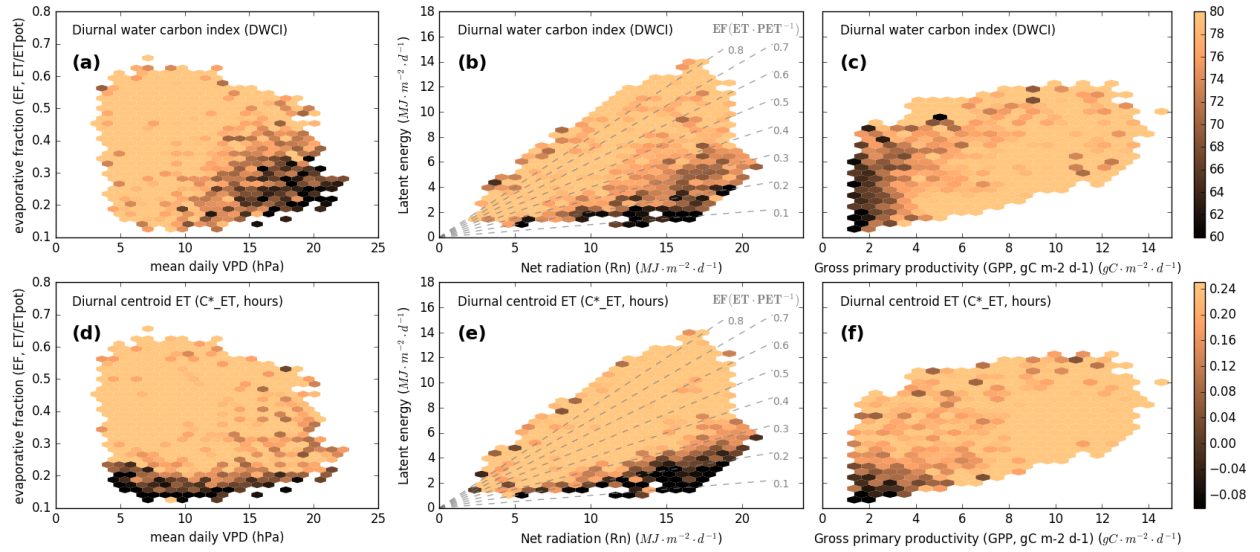


Figure 6: Mean DWCI (upper panels) and C_{ET}^* (lower panels) with respect to evaporative fraction (EF) by vapor pressure deficit VPD (a,d), latent energy (LE) by Rn (b,e) and LE by GPP (c,g). Note DWCI of 0-100 indicate lowest-highest probability of diurnal carbon:water coupling and C_{ET}^* of -1 to 1 indicate one hour morning shifted to one hour afternoon shifted ET. Points with high Rn and low LE are associated with both low DWCI and C_{ET}^* , indicating that both metrics are related to water limitations. Though both metrics are associated with low EF, DWCI shows a much higher response to atmospheric demand as measured by VPD, with C_{ET}^* showing very limited response. Both metrics, and DWCI in particular, show low values with high ET and low Rn, though these points are also associated with over closed energy balances ($LE+H>Rn$). Both metrics are associated with low GPP, but the C_{ET}^* is restricted to both low GPP and ET, indicating water and carbon can decouple over a wider range of water stress. This also holds when points with energy balance over-closer are excluded (data not shown).

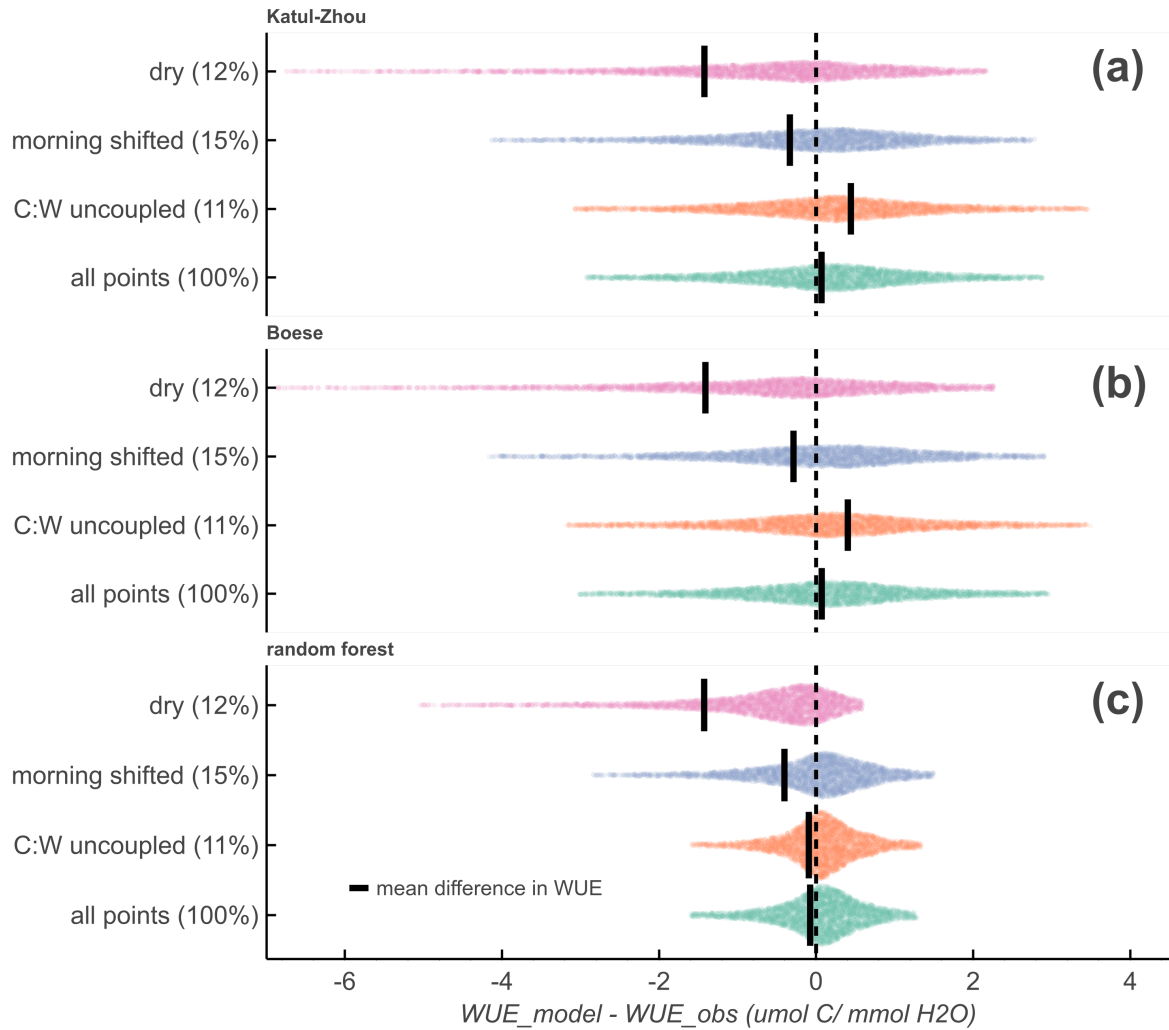


Figure 7: Difference in modeled and measured WUE for Katul-Zhou (a), Boese (b), and random forest (c) models. The random forest model was fit using R_g , VPD, T_{air} , GPP, and year. Thresholds designating dry, morning shifted, and C:W uncoupled days were $EF < 0.2$, $C_{ET}^* < -0.25$, and $DWCI < 25$ respectively for each day. The distributions span from the 5th to 95th percentiles, and the width of each gives an indication of the variance, which is larger in the sub groups compared to all points. Furthermore, the mean difference in WUE (black lines) tends to be shifted in dry and morning shifted days indicating a mean underestimation of WUE by the models mostly due to the long tails. Decoupled days show higher variance, but no clear pattern in under- or over-estimation. The percentage of days in each category are designated next to y-axis label in parenthesis.

287 Figure 7 shows the difference between expected and observed WUE from the Katul-Zhou, Boese, and random forest (RF)
 288 models, with respect to conditions of drought as characterized by low evaporative fraction ($EF < 0.2$), C:W decoupling
 289 ($DWCI < 25$), and morning shifts ($C_{ET}^* < -0.25$). This exercise was designed to test whether the metrics were associated
 290 with bias in the models, indicating that the metrics are able to capture information that the models are not (as further
 291 outlined in Methods and Materials subsection “models and parameter estimation”). For all models, the dry days show
 292 the largest average shift between expected and observed WUE, followed by morning shifted days. Uncoupled days show

293 the smallest shifts for all models, with an overestimation of WUE for the Katul-Zhou and Boese models and no significant
294 shift of WUE with the random forest model. As all models were calibrated within a site-year, the over or under estimation
295 of WUE indicate an inability of the model to capture a change in the system. Cases of mean mis-estimation tended to be
296 influenced by long tails in the distribution with median differences being less exaggerated. However, these long tails are
297 indicative of major model error in periods where the ecosystem is likely under stress conditions.

298 **Discussion**

299 **Looking beyond sums and means**

300 The proposed metrics, DWCI and C_{ET}^* , depart from more traditional methods to summarize from sub-daily to daily
301 timescales such as sums and means. This departure is advantageous in that it extracts added information that may have
302 been otherwise ignored by turning the focus from signal amplitude to the signal shape. However, these new metrics also
303 come with their own set of caveats, most notably issues with data quality confounding interpretability. Both metrics are
304 susceptible to noise, as one or two errant points within a day can be reflected as a decrease in correlation or a shift in
305 diurnal centroid. This is evident from the existence of very afternoon shifted C_{ET}^* , sometimes by more than an hour,
306 which the authors have no proposed explanation for other than noise in the data. However, attributing highly afternoon
307 shifted points as poor data requires further investigation. Note here that the “resting” C_{ET}^* seems to be slightly after-
308 noon shifted, which could be caused by real physiological factors such as differences in the incoming SW radiation (Rg)
309 used in the calculation and net radiation (Rn), higher atmospheric demand (VPD) in the afternoon driving higher ET,
310 or increased convection throughout the day resulting in higher transport of water away from the canopy, and is likely a
311 combination of all three. Differences in resting C_{ET}^* between sites could also be from instrumental causes such as ra-
312 diometric sensors which are not adequately leveled or dirty, though the consistent, slight afternoon shifts would suggest
313 this is a real response. Despite the possible shortcomings, both metrics show a definite response to drought conditions
314 across the broad array of sites, climates, and ecosystems contained in FLUXNET (see Figure 6), and give valuable in-
315 sight into the underlying physiology. Given the broad nature of the analysis here, the metrics and hypothesis presented
316 would benefit from site specific validations such as looking to see if the morning shifts and decoupling are indeed asso-
317 ciated with lower soil moisture levels, leaf water potentials, and/or decreases in sap flux. Sap flux in particular could
318 give some interesting insights, as the diurnal patterns in sap flux velocity will also have an offset to incoming radiation
319 related to tree capacitance, therefore relating sap flow diurnal centroids to the ET diurnal centroid could give some infor-
320 mation on changes in plant water recharge. Furthermore, the diurnal centroid base metrics complement the hysteresis
321 quantification methods such as those employed by Zhou et al. [54] and Matheny et al. [29], with the advantage of C_{ET}^*
322 being compensated for cloudy conditions and possibly comparatively less influence of noise, though an intercomparison

323 would be useful to explore the strengths and weaknesses of the different approaches. By providing both the equations
324 and related code of the metrics, we the authors hope the metrics will be used by the community for both validation and
325 to further ecophysiological understanding.

326 **Trees, grass, and drought stress**

327 By comparing climate groups and PFTs with the frequent occurrence of low DWCI and C_{ET}^* from Figure 4, we can note
328 two striking differences: evergreen broad- and needle-leaf forests show high variability of morning shifted days but not
329 uncoupled days, whereas grasslands show significantly high uncoupled but not morning shifted days. The pattern is
330 further seen in Figure 5, where the distinct divergent responses of decoupling and morning shifts between tree and grass
331 dominated systems. This disparity may indicate an interaction of C_{ET}^* not only with drought, but hydraulic sensitivity.
332 The association of morning shifts to hydraulic sensitivity is further strengthened by Figure 6a,d where C_{ET}^* shows a much
333 stronger response to EF rather than VPD, indicating that morning shifts of ET are not simply due to stomatal closure
334 due to VPD but in fact a response to drought conditions. The shorter hydraulic system of grasses may not necessitate
335 stomatal closure under high demands [14], thus causing less frequent phase shifts even under drought conditions. In
336 contrast, tree ecosystems may only exhibit higher hydraulic stresses, associated with both dryness and a more sensitive
337 hydraulic strategy. Temperate-continental and tropical climates all showed a low frequency of morning shifted days,
338 even though they are occupied by large trees with cavitation susceptible vascular systems [21], suggesting that these
339 ecosystems show limited drought stress even with the hydraulic susceptibility. Similarly, the high degree of variability
340 of morning shifted frequency between site-years in sub-tropical/Mediterranean and evergreen broad- and needle-leaf
341 forests could either indicate variation in the response in hydraulic stress between sites, or that hydraulic stress is only
342 expressed some years, leading to high and low frequencies within the same site.

343 In this way, it seems that though C_{ET}^* is less noisy as a drought indicator (see Figure 6), it may only be of use in tree
344 systems that are more prone to hydraulic stress. However, this does put the metric in a rather unique position in that it
345 could be used as a global scale hydraulic indicator, having potential application in exploring ecosystem level isohydricity
346 [27], or the degree to which risks vascular system damage to continue to extract water. Isohydricity is intrinsically a
347 concept that relates to an individual plant, as dynamics of rooting depth, hydraulic conductances, and sensitivities to
348 VPD can vary within individuals of the same species at the same location. However, these factors are all interrelated,
349 as hydraulic and stomatal conductances drive transpiration dynamics which control the rate of depletion of root zone
350 water which can then feed back to stomatal sensitivity, such as via ABA signaling [49]. As such, current estimates of
351 isohydricity require plant level measurements, which are currently restrained to the individual scale, i.e. from actual leaf
352 measurements [28] or to global scale, but only 0.5 degree resolution estimates from radar [21]. This limitation of large
353 and small scales leaves a knowledge gap at the size of an eddy covariance footprint, hindering the study of ecosystem

354 response to drought. However, under the assumption that the morning shifts seen under low evaporative fraction are
355 related to increased stomatal sensitivity in response to root zone moisture depletion, it may be possible to compare the
356 onset and speed with which the diurnal centroid shifts toward the mornings as ecosystems dry. In this way, one could
357 infer the ecosystem response to soil moisture, without explicitly knowing the soil moisture. The resulting relationship
358 could prove useful as a data derived ecosystem functional property, giving direct information on variations in water
359 limitation response.

360 **C:W decoupling and energy balance closure**

361 In addition to error from single data points, both metrics, but especially the DWCI, show some relationship with energy
362 balance over closure. Energy balance mismatch is a common phenomenon in EC measurements, with under closure
363 ($ET+H < R_n$) being a more common concern [24, 51]. Issues with energy balance closure can be, among other causes,
364 attributed to advection, where energy, water, and carbon are transported in and out of the tower footprint, complicating
365 an absolute accounting of these quantities [1, 5, 50]. The apparent association of DWCI and over closure could be due to
366 transfer of moist air from the surrounding landscape, causing the DWCI to be more contingent on the mixing of source
367 air and less from plant controls. In this scheme, the over closure seen in Figure 6 could be caused by the mixing of outside
368 moist air into the drier air from the EC site, causing an increase in latent energy. However, the infiltrating air sources
369 could also have similar or drier moisture levels which would not necessarily be seen as over closure. In this scenario, this
370 infiltrating air could contain varying carbon and water concentrations, again causing a carbon:water decoupling, but one
371 that would not be associated with over closure. If this effect has no diurnal pattern, and thus does not generally influence
372 the mean diurnal centroid in ET, it could explain why the patterns with dryness are much clearer with C_{ET}^* compared to
373 DWCI. This would have the implication that DWCI is then a mixture of advection and non-stomatal signals, complicating
374 the biological interpretability. However, the association with dryness in both metrics gives credence that they do indeed
375 reflect some physiology, if we assume EBC should not be influenced by dryness level. Furthermore, if potential stress
376 conditions are removed, the DWCI could be useful as a metric of advection in the system, even when the energy balance
377 is relatively well closed.

378 **WUE shifts associated with metrics and not captured by models**

379 Figure 7 demonstrates the strong tendency of the models to underestimation WUE in dry conditions. This is true even for
380 the fully non-linear and empirical random forest model, indicating that the model under-performance is not necessarily
381 due to an incomplete model framework, but due to a lack of information to constrain the problem. Given the association
382 of both metrics with drought (Figure 6), one could expect that the models would underestimate WUE in uncoupled and

383 morning shifted days. Though this is the case with morning shifted days, decoupling shows no underestimations of WUE,
384 with even a mean overestimation in the case of the Katul-Zhou and Boese models. Given the limitations outlined in the
385 previous sections, one could blame noise for the lack of WUE shift, but this does not reconcile with the higher frequency
386 of decoupling during dry days which should bias the WUE estimates. Furthermore, as the more empirical random forest
387 model reduces the prediction variability, leaving a slight WUE underestimation, indicating that some of the overestima-
388 tion from the Katul-Zhou and Boese models may be tied to limitations of the underlying assumptions, yet the distribution
389 from the RF model still lacks the long tails of underestimation characteristic of the dry points. Extending these findings
390 to the underlying hypotheses of the metrics, namely hydraulic and non-stomatal limitations, we could conclude that the
391 hydraulic controls do impose a greater water use advantage than non-stomatal limitations. In other words, the findings
392 suggest that days with water:carbon decoupling, and possibly non-stomatal limitations, do not improve WUE, whereas
393 hydraulic responses can improve WUE. As WUE is a ratio, this does not shed any light onto the change in productivity,
394 as low values of WUE may indicate that a plant is still productive, but at a higher water cost. However, solid conclusions
395 would require further analysis with some site specific measurements of actual plant function.

396 Though the models used here are relatively simple and lack the complexities and feedbacks found in more vigorous
397 ecosystem models, Matheny et al. [29] also demonstrated the fundamental inability of 9 different land-surface models
398 with 4 different stomatal conductance schemes to capture diurnal variability which the authors attributed to inadequate
399 representation of how water gets from the soil to the leaf. Given the demonstrated phenomenon of morning shifts and
400 decoupling across sites under dry conditions, the metrics here provide a benchmarking tool for mechanistic models to
401 test their ability to replicate these patterns, suggesting that the models are capable of expressing hydraulic and non-
402 stomatal limitations. Furthermore, in the case of machine learning approaches, the metrics may provide a useful input
403 parameter which summarizes these diurnal effects, as is evidence by the difference in response the bias in RF modeled
404 WUE, i.e. while both metrics are associated with low EF, RF WUE was underestimated with morning shifted days but not
405 decoupled days implying that two different strategies are being captured by the metrics. As such, by demonstrating the
406 utility of the metrics, and providing code and explanations for calculation, we hope they become useful to the community
407 at large.

408 **Conclusion**

409 Both the DWCI and the C_{ET}^* demonstrate an ability to show consistent patterns with drought across a broad array
410 of sites, climates, and ecosystems, with the added advantage of being tied to theoretical underpinnings. Particularly,
411 the demonstrated patterns give novel information about carbon water relations and hydrological dynamics that are not
412 currently present at ecosystem scale across a database as large as FLUXNET. These metrics and their underlying theory
413 provide a data derived example differentiating the hydrological response of tree and grass plant functional types, as well

414 as give evidence for the presence and absence of a WUE advantage from hydraulic and stomatal limitations respectively.
415 Going forward, these metrics can be used as a tool to further understand the diversity of ecosystem drought responses.

416 **References**

- 417 [1] A.G. Barr et al. “Surface energy balance closure by the eddy-covariance method above three boreal forest stands
418 and implications for the measurement of the CO₂ flux”. en. In: *Agricultural and Forest Meteorology* 140.1-4 (Nov.
419 2006), pp. 322–337. ISSN: 01681923. DOI: 10.1016/j.agrformet.2006.08.007. URL: <http://linkinghub.elsevier.com/retrieve/pii/S0168192306002292> (visited on 11/25/2016).
- 421 [2] C. Beer et al. “Temporal and among-site variability of inherent water use efficiency at the ecosystem level:
422 VARIABILITY OF INHERENT WUE”. en. In: *Global Biogeochemical Cycles* 23.2 (June 2009), n/a–n/a. ISSN:
423 08866236. DOI: 10.1029/2008GB003233. URL: <http://doi.wiley.com/10.1029/2008GB003233> (visited on
424 02/12/2016).
- 425 [3] Sven Boese et al. “The importance of radiation for semi-empirical water-use efficiency models”. en. In: *Biogeo-*
426 *sciences Discussions* (Jan. 2017), pp. 1–22. ISSN: 1810-6285. DOI: 10.5194/bg-2016-524. URL: <http://www.biogeosciences-discuss.net/bg-2016-524/> (visited on 01/09/2017).
- 428 [4] Leo Breiman. “Random forests”. In: *Machine learning* 45.1 (2001), pp. 5–32. URL: <http://link.springer.com/article/10.1023/A:1010933404324> (visited on 11/03/2016).
- 430 [5] Björn Brötz et al. “Early-Morning Flow Transition in a Valley in Low-Mountain Terrain Under Clear-Sky Con-
431 ditions”. en. In: *Boundary-Layer Meteorology* 152.1 (July 2014), pp. 45–63. ISSN: 0006-8314, 1573-1472. DOI:
432 10.1007/s10546-014-9921-7. URL: <http://link.springer.com/10.1007/s10546-014-9921-7> (visited on
433 11/25/2016).
- 434 [6] Ph. Ciais et al. “Europe-wide reduction in primary productivity caused by the heat and drought in 2003”. en. In:
435 *Nature* 437.7058 (Sept. 2005), pp. 529–533. ISSN: 0028-0836, 1476-4687. DOI: 10.1038/nature03972. URL:
436 <http://www.nature.com/articles/nature03972> (visited on 01/16/2018).
- 437 [7] Gaëlle Damour et al. “An overview of models of stomatal conductance at the leaf level: Models of stomatal con-
438 ductance”. en. In: *Plant, Cell & Environment* (July 2010), no–no. ISSN: 01407791, 13653040. DOI: 10.1111/j.1365-
439 3040.2010.02181.x. URL: <http://doi.wiley.com/10.1111/j.1365-3040.2010.02181.x> (visited on 07/07/2016).
- 440 [8] M. G. De Kauwe et al. “Do land surface models need to include differential plant species responses to drought?
441 Examining model predictions across a mesic-xeric gradient in Europe”. en. In: *Biogeosciences* 12.24 (Dec. 2015),

- 442 pp. 7503–7518. ISSN: 1726-4189. DOI: 10.5194/bg-12-7503-2015. URL: <http://www.biogeosciences.net/12/7503/2015/> (visited on 08/11/2016).
- 443
- 444 [9] Michael C. Dietze et al. “A quantitative assessment of a terrestrial biosphere model’s data needs across North
445 American biomes: PEcAn/ED model-data uncertainty analysis”. en. In: *Journal of Geophysical Research: Biogeo-*
446 *sciences* 119.3 (Mar. 2014), pp. 286–300. ISSN: 21698953. DOI: 10.1002/2013JG002392. URL: <http://doi.wiley.com/10.1002/2013JG002392> (visited on 09/16/2016).
- 447
- 448 [10] Gregorio Egea, Anne Verhoef, and Pier Luigi Vidale. “Towards an improved and more flexible representation of
449 water stress in coupled photosynthesis–stomatal conductance models”. en. In: *Agricultural and Forest Meteorol-*
450 *ogy* 151.10 (Oct. 2011), pp. 1370–1384. ISSN: 01681923. DOI: 10.1016/j.agrformet.2011.05.019. URL: <http://linkinghub.elsevier.com/retrieve/pii/S0168192311001778> (visited on 09/15/2016).
- 451
- 452 [11] Jaume Flexas et al. “Mesophyll diffusion conductance to CO₂: An unappreciated central player in photosynthesis”.
453 en. In: *Plant Science* 193-194 (Sept. 2012), pp. 70–84. ISSN: 01689452. DOI: 10.1016/j.plantsci.2012.05.009.
454 URL: <http://linkinghub.elsevier.com/retrieve/pii/S0168945212001069> (visited on 08/25/2016).
- 455 [12] *FLUXNET Data Download*. 2007. URL: <http://www.fluxdata.org/%20DataDownload/default.aspx> (visited on
456 06/08/2017).
- 457 [13] A. Granier et al. “Evidence for soil water control on carbon and water dynamics in European forests during the
458 extremely dry year: 2003”. en. In: *Agricultural and Forest Meteorology* 143.1-2 (Mar. 2007), pp. 123–145. ISSN:
459 01681923. DOI: 10.1016/j.agrformet.2006.12.004. URL: <http://linkinghub.elsevier.com/retrieve/pii/S0168192306003911> (visited on 01/16/2018).
- 460
- 461 [14] Meisha-Marika Holloway-Phillips and Timothy J. Brodribb. “Minimum hydraulic safety leads to maximum water-
462 use efficiency in a forage grass: Minimum hydraulic safety, maximum water-use efficiency”. en. In: *Plant, Cell &*
463 *Environment* 34.2 (Feb. 2011), pp. 302–313. ISSN: 01407791. DOI: 10.1111/j.1365-3040.2010.02244.x. URL:
464 <http://doi.wiley.com/10.1111/j.1365-3040.2010.02244.x> (visited on 11/29/2016).
- 465 [15] Akihiko Ito and Motoko Inatomi. “Water-Use Efficiency of the Terrestrial Biosphere: A Model Analysis Focusing
466 on Interactions between the Global Carbon and Water Cycles”. en. In: *Journal of Hydrometeorology* 13.2 (Apr.
467 2012), pp. 681–694. ISSN: 1525-755X, 1525-7541. DOI: 10.1175/JHM-D-10-05034.1. URL: <http://journals.ametsoc.org/doi/abs/10.1175/JHM-D-10-05034.1> (visited on 01/13/2017).
- 468
- 469 [16] Gabriel G. Katul, Sari Palmroth, and Ram Oren. “Leaf stomatal responses to vapour pressure deficit under current
470 and CO₂-enriched atmosphere explained by the economics of gas exchange”. en. In: *Plant, Cell & Environment*
471 32.8 (Aug. 2009), pp. 968–979. ISSN: 01407791, 13653040. DOI: 10.1111/j.1365-3040.2009.01977.x. URL:
472 <http://doi.wiley.com/10.1111/j.1365-3040.2009.01977.x> (visited on 10/24/2016).

- 473 [17] Gabriel Katul et al. “A stomatal optimization theory to describe the effects of atmospheric CO₂ on leaf photosyn-
474 thesis and transpiration”. en. In: *Annals of Botany* 105.3 (Mar. 2010), pp. 431–442. ISSN: 1095-8290, 0305-7364.
475 DOI: 10.1093/aob/mcp292. URL: <https://academic.oup.com/aob/article-lookup/doi/10.1093/aob/mcp292>
476 (visited on 01/11/2018).
- 477 [18] Trevor F. Keenan et al. “Increase in forest water-use efficiency as atmospheric carbon dioxide concentrations rise”.
478 In: *Nature* 499.7458 (July 2013), pp. 324–327. ISSN: 0028-0836, 1476-4687. DOI: 10.1038/nature12291. URL:
479 <http://www.nature.com/doi/10.1038/nature12291> (visited on 05/22/2015).
- 480 [19] Jürgen Knauer, Christiane Werner, and Sönke Zaehle. “Evaluating stomatal models and their atmospheric
481 drought response in a land surface scheme: A multibiome analysis: MULTIBIOME STOMATAL MODEL EVAL-
482 UATION”. en. In: *Journal of Geophysical Research: Biogeosciences* 120.10 (Oct. 2015), pp. 1894–1911. ISSN:
483 21698953. DOI: 10.1002/2015JG003114. URL: <http://doi.wiley.com/10.1002/2015JG003114> (visited on
484 01/12/2017).
- 485 [20] Roger Koenker and Gilbert Bassett Jr. “Regression quantiles”. In: *Econometrica: journal of the Econometric So-*
486 *ciety* (1978), pp. 33–50. URL: <http://www.jstor.org/stable/1913643> (visited on 02/06/2017).
- 487 [21] Alexandra G. Konings and Pierre Gentine. “Global variations in ecosystem-scale isohydrlicity”. en. In: *Global*
488 *Change Biology* (July 2016). ISSN: 13541013. DOI: 10.1111/gcb.13389. URL: [http://doi.wiley.com/10.1111/](http://doi.wiley.com/10.1111/gcb.13389)
489 [gcb.13389](http://doi.wiley.com/10.1111/gcb.13389) (visited on 09/16/2016).
- 490 [22] F. G. Kuglitsch et al. “Characterisation of ecosystem water-use efficiency of european forests from eddy covariance
491 measurements”. In: *Biogeosciences Discussions* 5.6 (2008), pp. 4481–4519.
- 492 [23] D. W. Lawlor and W. Tezara. “Causes of decreased photosynthetic rate and metabolic capacity in water-deficient
493 leaf cells: a critical evaluation of mechanisms and integration of processes”. en. In: *Annals of Botany* 103.4 (May
494 2008), pp. 561–579. ISSN: 0305-7364, 1095-8290. DOI: 10.1093/aob/mcn244. URL: [http://aob.oxfordjournals.](http://aob.oxfordjournals.org/cgi/doi/10.1093/aob/mcn244)
495 [org/cgi/doi/10.1093/aob/mcn244](http://aob.oxfordjournals.org/cgi/doi/10.1093/aob/mcn244) (visited on 08/25/2016).
- 496 [24] Ray Leuning et al. “Reflections on the surface energy imbalance problem”. en. In: *Agricultural and Forest Me-*
497 *teorology* 156 (Apr. 2012), pp. 65–74. ISSN: 01681923. DOI: 10.1016/j.agrformet.2011.12.002. URL: [http://](http://linkinghub.elsevier.com/retrieve/pii/S016819231100339X)
498 linkinghub.elsevier.com/retrieve/pii/S016819231100339X (visited on 03/17/2017).
- 499 [25] S. Manzoni. “Integrating plant hydraulics and gas exchange along the drought-response trait spectrum”. en. In:
500 *Tree Physiology* 34.10 (Oct. 2014), pp. 1031–1034. ISSN: 0829-318X, 1758-4469. DOI: 10.1093/treephys/tpu088.
501 URL: <http://treephys.oxfordjournals.org/cgi/doi/10.1093/treephys/tpu088> (visited on 10/28/2016).

- 502 [26] Stefano Manzoni et al. “Optimization of stomatal conductance for maximum carbon gain under dynamic soil
503 moisture”. en. In: *Advances in Water Resources* 62 (Dec. 2013), pp. 90–105. ISSN: 03091708. DOI: 10.1016/j.
504 advwatres.2013.09.020. URL: <http://linkinghub.elsevier.com/retrieve/pii/S0309170813001814> (visited on
505 01/12/2018).
- 506 [27] Jordi Martínez-Vilalta and Núria Garcia-Forner. “Water potential regulation, stomatal behaviour and hydraulic
507 transport under drought: deconstructing the iso/anisohydric concept: Deconstructing the iso/anisohydric con-
508 cept”. en. In: *Plant, Cell & Environment* (2016). ISSN: 01407791. DOI: 10.1111/pce.12846. URL: <http://doi.wiley.com/10.1111/pce.12846> (visited on 11/01/2016).
- 509 [28] Jordi Martínez-Vilalta et al. “A new look at water transport regulation in plants”. en. In: *New Phytologist* 204.1
510 (Oct. 2014), pp. 105–115. ISSN: 0028646X. DOI: 10.1111/nph.12912. URL: <http://doi.wiley.com/10.1111/nph.12912>
511 (visited on 06/01/2016).
- 512 [29] Ashley M. Matheny et al. “Characterizing the diurnal patterns of errors in the prediction of evapotranspiration
513 by several land-surface models: An NACP analysis: Error patterns in modeled transpiration”. en. In: *Journal*
514 *of Geophysical Research: Biogeosciences* 119.7 (July 2014), pp. 1458–1473. ISSN: 21698953. DOI: 10.1002/
515 2014JG002623. URL: <http://doi.wiley.com/10.1002/2014JG002623> (visited on 02/15/2016).
- 516 [30] Belinda E. Medlyn et al. “How do leaf and ecosystem measures of water-use efficiency compare?” en. In: *New*
517 *Phytologist* 216.3 (Nov. 2017), pp. 758–770. ISSN: 0028646X. DOI: 10.1111/nph.14626. URL: <http://doi.wiley.com/10.1111/nph.14626>
518 (visited on 01/19/2018).
- 519 [31] Belinda E. Medlyn et al. “Temperature response of parameters of a biochemically based model of photosynthesis.
520 II. A review of experimental data”. In: *Plant, Cell & Environment* 25.9 (2002), pp. 1167–1179.
- 521 [32] Mirco Migliavacca et al. “Seasonal and interannual patterns of carbon and water fluxes of a poplar plantation under
522 peculiar eco-climatic conditions”. en. In: *Agricultural and Forest Meteorology* 149.9 (Sept. 2009), pp. 1460–1476.
523 ISSN: 01681923. DOI: 10.1016/j.agrformet.2009.04.003. URL: [http://linkinghub.elsevier.com/retrieve/pii/
524 S0168192309000884](http://linkinghub.elsevier.com/retrieve/pii/S0168192309000884) (visited on 03/17/2017).
- 525 [33] Jacob A Nelson. *Jnelson18/Fluxnettools: Initial Release*. DOI: 10.5281/zenodo.1010483. Oct. 2017.
- 526 [34] Kimberly A. Novick, Chelcy F. Miniati, and James M. Vose. “Drought limitations to leaf-level gas exchange: results
527 from a model linking stomatal optimization and cohesion-tension theory: Drought limitations to gas exchange”.
528 en. In: *Plant, Cell & Environment* 39.3 (Mar. 2016), pp. 583–596. ISSN: 01407791. DOI: 10.1111/pce.12657. URL:
529 <http://doi.wiley.com/10.1111/pce.12657> (visited on 02/16/2016).
- 530

- 531 [35] Sari Palmroth et al. “On the complementary relationship between marginal nitrogen and water-use efficiencies
532 among *Pinus taeda* leaves grown under ambient and CO₂-enriched environments”. en. In: *Annals of Botany* 111.3
533 (Mar. 2013), pp. 467–477. ISSN: 1095-8290, 0305-7364. DOI: 10.1093/aob/mcs268. URL: [https://academic.
534 oup.com/aob/article-lookup/doi/10.1093/aob/mcs268](https://academic.oup.com/aob/article-lookup/doi/10.1093/aob/mcs268) (visited on 01/12/2018).
- 535 [36] Dario Papale et al. “Towards a standardized processing of Net Ecosystem Exchange measured with eddy covari-
536 ance technique: algorithms and uncertainty estimation”. In: *Biogeosciences* 3.4 (2006), pp. 571–583. URL: <https://hal.archives-ouvertes.fr/hal-00330317/>
537 (visited on 11/07/2016).
- 538 [37] Fabian Pedregosa et al. “Scikit-learn: Machine learning in Python”. In: *Journal of Machine Learning Research*
539 12.Oct (2011). bibtex: pedregosa_scikit-learn_2011, pp. 2825–2830. URL: [http://www.jmlr.org/papers/v12/
540 pedregosa11a.html](http://www.jmlr.org/papers/v12/pedregosa11a.html) (visited on 11/03/2016).
- 541 [38] C. H. B. Priestley and R. J. Taylor. “On the assessment of surface heat flux and evaporation using large-scale
542 parameters”. In: *Monthly weather review* 100.2 (1972), pp. 81–92.
- 543 [39] M. Reichstein et al. “Reduction of ecosystem productivity and respiration during the European summer 2003
544 climate anomaly: a joint flux tower, remote sensing and modelling analysis”. en. In: *Global Change Biology* 13.3
545 (Mar. 2007), pp. 634–651. ISSN: 1354-1013, 1365-2486. DOI: 10.1111/j.1365-2486.2006.01224.x. URL: <http://doi.wiley.com/10.1111/j.1365-2486.2006.01224.x>
546 (visited on 01/16/2018).
- 547 [40] Markus Reichstein. “Inverse modeling of seasonal drought effects on canopy CO₂ /H₂O exchange in three
548 Mediterranean ecosystems”. en. In: *Journal of Geophysical Research* 108.D23 (2003). ISSN: 0148-0227. DOI:
549 10.1029/2003JD003430. URL: <http://doi.wiley.com/10.1029/2003JD003430> (visited on 09/28/2015).
- 550 [41] Markus Reichstein et al. “On the separation of net ecosystem exchange into assimilation and ecosystem
551 respiration: review and improved algorithm”. en. In: *Global Change Biology* 11.9 (Sept. 2005). bibtex: reich-
552 stein_separation_2005, pp. 1424–1439. ISSN: 1354-1013, 1365-2486. DOI: 10.1111/j.1365-2486.2005.001002.x.
553 URL: <http://doi.wiley.com/10.1111/j.1365-2486.2005.001002.x> (visited on 11/07/2016).
- 554 [42] Markus Reichstein et al. “Severe drought effects on ecosystem CO₂ and H₂O fluxes at three Mediterranean ever-
555 green sites: revision of current hypotheses?” In: *Global Change Biology* 8.10 (2002), pp. 999–1017. ISSN: 1365-
556 2486. DOI: 10.1046/j.1365-2486.2002.00530.x. URL: <http://dx.doi.org/10.1046/j.1365-2486.2002.00530.x>.
- 557 [43] Sascha Reth, Markus Reichstein, and Eva Falge. “The effect of soil water content, soil temperature, soil pH-value
558 and the root mass on soil CO₂ efflux – A modified model”. en. In: *Plant and Soil* 268.1 (Jan. 2005), pp. 21–33. ISSN:
559 0032-079X, 1573-5036. DOI: 10.1007/s11104-005-0175-5. URL: [http://link.springer.com/10.1007/s11104-005-
560 0175-5](http://link.springer.com/10.1007/s11104-005-0175-5) (visited on 02/15/2016).

- 561 [44] Alistair Rogers et al. “A roadmap for improving the representation of photosynthesis in Earth system models”. In:
562 *New Phytologist* 213.1 (2017), pp. 22–42. URL: <http://onlinelibrary.wiley.com/doi/10.1111/nph.14283/full>
563 (visited on 01/03/2017).
- 564 [45] Peter J. Rousseeuw. “Regression techniques with high breakdown point”. In: *The Institute of Mathematical Statis-*
565 *tics Bulletin* 12 (1983), p. 155.
- 566 [46] William H. Schlesinger and Scott Jasechko. “Transpiration in the global water cycle”. en. In: *Agricultural and*
567 *Forest Meteorology* 189-190 (June 2014), pp. 115–117. ISSN: 01681923. DOI: 10.1016/j.agrformet.2014.01.011.
568 URL: <http://linkinghub.elsevier.com/retrieve/pii/S0168192314000203> (visited on 05/22/2015).
- 569 [47] Xuguang Tang et al. “How is water-use efficiency of terrestrial ecosystems distributed and changing on Earth?” In:
570 *Scientific Reports* 4 (Dec. 2014), p. 7483. ISSN: 2045-2322. DOI: 10.1038/srep07483. URL: <http://www.nature.com/articles/srep07483> (visited on 01/12/2017).
- 571
- 572 [48] Melvin T. Tyree and John S. Sperry. “Do woody plants operate near the point of catastrophic xylem dysfunction
573 caused by dynamic water stress? Answers from a model”. In: *Plant physiology* 88.3 (1988), pp. 574–580. URL:
574 <http://www.plantphysiol.org/content/88/3/574.short> (visited on 02/16/2017).
- 575 [49] S. Wilkinson and W. J. Davies. “ABA-based chemical signalling: the co-ordination of responses to stress in plants”.
576 en. In: *Plant, Cell and Environment* 25.2 (Feb. 2002), pp. 195–210. ISSN: 0140-7791, 1365-3040. DOI: 10.1046/
577 j.0016-8025.2001.00824.x. URL: <http://doi.wiley.com/10.1046/j.0016-8025.2001.00824.x> (visited on
578 01/20/2018).
- 579 [50] Kell B. Wilson et al. “Diurnal centroid of ecosystem energy and carbon fluxes at FLUXNET sites: DIURNAL
580 ENERGY FLUXES AT FLUXNET SITES”. en. In: *Journal of Geophysical Research: Atmospheres* 108.D21 (Nov.
581 2003). ISSN: 01480227. DOI: 10.1029/2001JD001349. URL: <http://doi.wiley.com/10.1029/2001JD001349>
582 (visited on 06/13/2016).
- 583 [51] Kell Wilson et al. “Energy balance closure at FLUXNET sites”. In: *Agricultural and Forest Meteorology* 113.1
584 (2002), pp. 223–243. URL: <http://www.sciencedirect.com/science/article/pii/S0168192302001090> (visited on
585 03/17/2017).
- 586 [52] Sha Zhou et al. “Daily underlying water use efficiency for AmeriFlux sites: DAILY UNDERLYING WUE”. en. In:
587 *Journal of Geophysical Research: Biogeosciences* 120.5 (May 2015), pp. 887–902. ISSN: 21698953. DOI: 10.1002/
588 2015JG002947. URL: <http://doi.wiley.com/10.1002/2015JG002947> (visited on 02/18/2016).
- 589 [53] Sha Zhou et al. “Partitioning evapotranspiration based on the concept of underlying water use efficiency: ET PAR-
590 TITIONING”. en. In: *Water Resources Research* 52.2 (Feb. 2016). bibtex: zhou_partitioning_2016, pp. 1160–1175.

591 ISSN: 00431397. DOI: 10.1002/2015WR017766. URL: <http://doi.wiley.com/10.1002/2015WR017766> (visited
592 on 06/13/2016).

593 [54] Sha Zhou et al. “The effect of vapor pressure deficit on water use efficiency at the subdaily time scale: Underlying
594 water use efficiency”. en. In: *Geophysical Research Letters* 41.14 (July 2014), pp. 5005–5013. ISSN: 00948276.
595 DOI: 10.1002/2014GL060741. URL: <http://doi.wiley.com/10.1002/2014GL060741> (visited on 02/16/2016).

596 [55] Shuangxi Zhou et al. “How should we model plant responses to drought? An analysis of stomatal and non-stomatal
597 responses to water stress”. en. In: *Agricultural and Forest Meteorology* 182-183 (Dec. 2013), pp. 204–214. ISSN:
598 01681923. DOI: 10.1016/j.agrformet.2013.05.009. URL: [http://linkinghub.elsevier.com/retrieve/pii/
599 S0168192313001263](http://linkinghub.elsevier.com/retrieve/pii/S0168192313001263) (visited on 10/28/2016).